It is evident from the results in Fig. 4 that steady-state waves corresponding to the first and third modes can exist in the boundary layer. As for the second mode, it undergoes upstream attenuation by relaxation in the limit $\omega \to 0$.

LITERATURE CITED

1. C. C. Lin, The Theory of Hydrodynamic Stability, 2nd ed., Cambridge Univ. Press, Oxford (1966).
2. A. Demetriades, "An experiment on the stability of hypersonic laminar boundary layers," J. Fluid Mech., 7, Part 3 (1960).
3. J. Laufer and T. Vrebalovich, "Stability and transition of a supersonic laminar boundary layer on an insulated flat plate," J. Fluid Mech., 9, Part 2 (1960).
4. J. M. Kendall, "Supersonic boundary-layer stability experiments," in: Proceedings of the Boundary-Layer Transition Study Group Meeting, Air Force Rep. N BSD-TR-67-213 (1967).
5. A. D. Kosinov and A. A. Maslov, "Growth of artificially induced disturbances in a supersonic boundary layer," Izv. Akad. Nauk SSSR, Mekh. Zhidk. Gaza, No. 5 (1984).
6. S. A. Gaponov, "Influence of flow nonparallelism on the growth of disturbances in a supersonic boundary layer," Izv. Akad. Nauk SSSR, Mekh. Zhidk. Gaza, No. 2 (1980).
7. A. D. Kosinov, A. A. Maslov, and S. G. Shevel'kov, "Experimental study of the wave structure of a supersonic boundary layer," Zh. Prikl. Mekh. Tekh. Fiz., No. 5 (1986).
8. A. D. Kosinov, A. A. Maslov, and S. G. Shevel'kov, "Experimental study of the growth of disturbances in the boundary layer of a flat plate at Mach number M = 4.0," Izv. Akad. Nauk SSSR, Mekh. Zhidk. Gaza, No. 6 (1990).
9. S. A. Gaponov and A. A. Maslov, Growth of Disturbances in Compressible Flows [in Russian], Nauka, Novosibirsk (1980).
10. S. A. Gaponov, "Growth of three-dimensional disturbances in a slightly nonparallel supersonic flow," Izv. Sib. Otd. Akad. Nauk SSSR Tekh. Nauk, No. 3, Part 1 (1982).
11. S. A. Gaponov and V. I. Lysenko, "Growth of disturbances near a surface in supersonic flow," Zh. Prikl. Mekh. Tekh. Fiz., No. 6 (1988).

FEATURES OF SEPARATED SUPERSONIC FLOW PULSATIONS AHEAD OF A SPIKE-TIPPED CYLINDER

V. I. Zapryagaev and S. G. Mironov

UDC 534.13:533.6.011.5

Use of a spike on a blunt body to decrease the aerodynamic resistance is limited by the adverse effect of intense flow pulsations, which depend on the shape of the front end of the body, the length of the spike, and the Mach number of the flow. Supersonic pulsation flow around such configurations have been investigated [1-7]. The intensive pulsations are excited by autooscillations in the forward separation zone ahead of the end with the spike.

The autooscillation system has distributed parameters; modeling it mathematically is a complex problem. The trend to construct simplified models makes it necessary to distinguish the most important components of the system: the oscillation system itself, the element which controls the input of energy into the system, feedback, and the energy source (the high-velocity flow) which surrounds the separation zone [8]. Delineating the basic elements of the autooscillation system requires detailed investigation, not only of the spectral and correlation characteristics of the pulsations, but also the separate stages of the flow pattern.

Experimental data on the magnitude and spectral composition of pressure pulsations on a cylinder with a conical spike, which has a 20° half-angle, are presented in [7], along with a preliminary discussion of the pulsation mechanism. Here we refine the description of the pulsation mechanism on a cylinder with a spike. We also give experimental data on

---

Novosibirsk. Translated from Prikladnaya Mekhanika i Tekhnicheskaya Fizika, No. 6, pp. 101-108, November-December, 1991. Original article submitted February 9, 1990; revision submitted June 21, 1990.

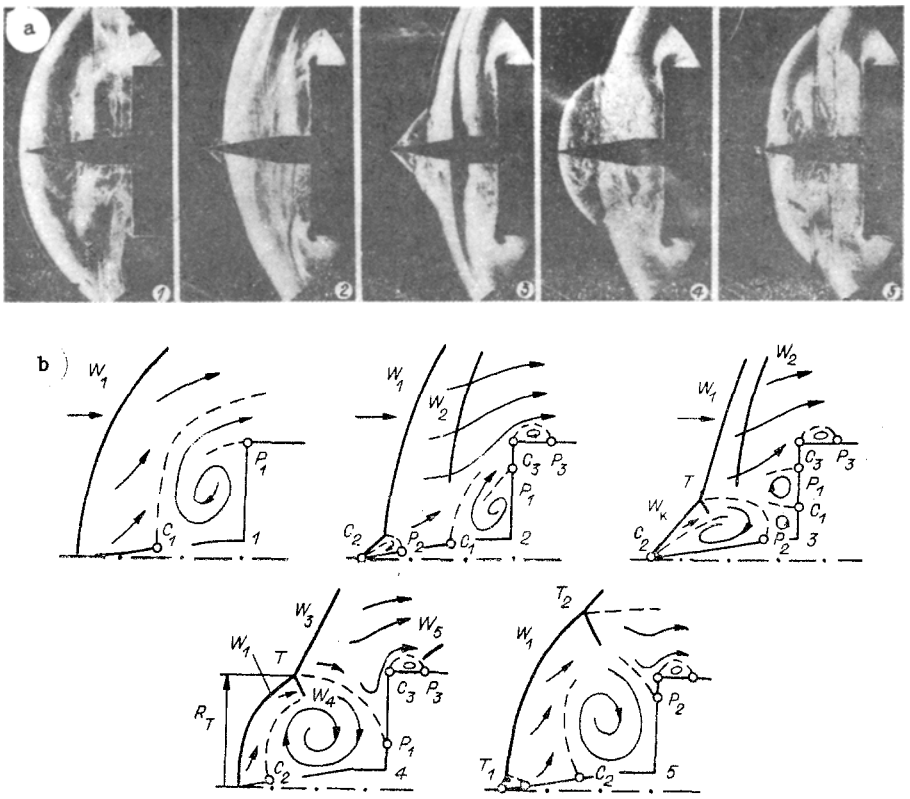

Fig. 1

the character of the pulsations for a spike whose length has the same dimensions as the distance to the separated shock wave.

1. Experiments were conducted on a model, which was a cylinder of diameter D = 100 mm. On the end of the cylinder was fastened a spike, which was a cylinder of diameter d with a conical tip of half-angle θ (d = 4 or 16 mm). The length of the spike was varied in discrete steps in the range $\bar{l} = l/D = 0\text{-}1.5$. Four piezometric transducers to measure the pulsation pressure were fastened on the end of the cylinder in a circle of diameter $0.76 \cdot D$. The tests were conducted with cold air at a zero angle of attack ($T_{00} \approx 280$ K) in a supersonic wind tunnel [9] for flow Mach numbers $M_\infty = 2.0$ and 3.0. The Reynolds number, obtained from the incoming flow parameters and the cylinder diameter was $Re_\infty = (2.4\text{-}5.0) \cdot 10^6$. In order to measure the statistical characteristics of the pressure pulsations, signals from the transducers were sent to a single-channel N067 recording magnetometer and processed later. The nature of the shock-wave motion was determined by relating instantaneous photographs of the flow field to measured pressure pulsations [10].

2. Intensive pulsations of the separation flow in the forward part of the cylinder arise when the length of the spike is larger than the axial distance from the end of the cylinder to the separated curvilinear shock wave in the absence of a spike. The ratio of the root mean square value of the pressure pulsation p_Σ to the velocity head q_∞ of the external flow lies in the range of 0.3-1.0. Data from [1] indicate that for $M_\infty = 3.0$, and $Re_1 = 7 \cdot 10^6$ m^{-1} (Re_1 is the unit Reynolds number), the maximum $p_\Sigma/q_\infty = 0.82$.

A series of peaks are observed in the frequency spectrum of the intense pressure pulsations [1, 7]. From our measurements, the Strouhal number of the basic frequency is described satisfactorily by the empirical relationship

$$\mathrm{Sh} = fl/u_\infty = -0{,}1\bar{l}^2 + 0{,}38\bar{l} - 0{,}07. \qquad (2.1)$$

Equation (2.1) can be used with an accuracy up to 25% in the range $0.4 \leq \bar{l} \leq 1.5$ and $M_\infty = 2\text{-}3$ for $Re_\infty = (2.4\text{-}3.3) \cdot 10^6$ for an aperture half-angle at the spike of $\theta = 10\text{-}45°$. Similar values of the frequency are given in [4].

Measured correlation functions indicated in-phase pressure pulsations for all transducers on the end of the cylinder. The shape of the pressure pulsation oscillograms depend on the shape of the spike tip and its length.

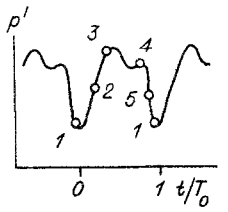

Fig. 2

3. Two pulsation regimes were noted in the observed pulsations in the forward separation zone on the body with the spike [5, 6]. These regimes have been called [7] mass dissipation pulsations and acoustic oscillations. The first regime is realized for a short spike; the second for a longer one. The term "acoustical oscillations" is taken to mean oscillations whose mechanism is similar to the mechanism of pulsations in the streamlines surrounded by the flow. The basis of the latter mechanism is the instability of the shear layer above the streamlines. The feedback in this case is closed by means of the acoustic waves which are propagated in the channel (see [11], for example). The criterion which delimits the pulsations between mass dissipation and acoustic, is given in [7]. The description in the literature of mass dissipation pulsations, as applied to a blunt body with a spike, have not been developed fully enough to define a mathematical model. Therefore, at this point we present a mechanism for mass dissipation pulsations for supersonic flow around a cylinder with a sharp spike, whose main feature is the intensive mass transfer near the outer boundary of the cylinder. In constructing this method, along with available experimental data, we use the results of numerical calculations of a similar pulsation flow [2] and an experimental investigation of the flow structure ahead of a two-dimensional step [12].

The schlieren photographs in Fig. 1a and the corresponding flow diagrams (Fig. 1b) for various stages of the pulsations correspond to $M_\infty = 2.0$, $Re_\infty = 2.5 \cdot 10^6$, $\bar{d} = d/D = 0.16$, $\bar{\ell} = 0.65$, and $\theta = 10°$. An oscillogram of the pressure pulsations $p'(t/T_0)$ is presented in Fig. 2. The points 1-5 in the oscillogram correspond to the times in the photographs and the flow diagrams. The root mean square of the deviation of the pulsation period from its average value reaches 5%, which gives the error in determining the actual stage at the moment the photographs were taken.

We will start to examine the autooscillations at the time ($t = 0$) at which the minimum pressure is recorded on the end of the cylinder. This stage corresponds to the maximum withdrawal of the main shock wave W_1 from the end. The use of the term shock wave (and not shock front) is dictated by the significant displacement velocity of the wave, which is observed at separate moments of time. At $t = 0$, the shape of the shock wave is close to that of a wave which forms for flow around a blunt body without a spike. However, this shock wave is located farther from the end than is the case when there is no nose spike. The shock wave is not displaced for this stage of pulsations. This distribution of the main shock wave is explained by the fact that, at a given time, the stall zone plays the role of the blunt body and the spike is surrounded by subsonic flow. In photo 1, we can clearly see the boundary separating the gas directly behind the shock wave and the turbulent gas flowing into the vortex motion of the separation zone. In diagram 1, this separation line starts from the point C_1. The streamlines of the incoming flow, which pass through the wave W_1, are shown based on the assumption that a fluid contour, limited by these separating stream lines, flows around them. A similar shock wave distribution relative to the body is unstable, which is manifested by the evacuation of the separation zone. The separating streamline, which comes to the point P_1 is constructed from the fact that vortex flow must exist in the separation zone in front of the end [of the cylinder]. As the separation zone decreases, part of the gas flows outwards, and part remains inside the separation zone.

For this pulsation stage, the outflow from the separation zone dominates some incoming mass of gas, due to the mass transfer within the separation zone through the separating streamline (shear layer), which starts from the point C_1. The decrease in the gas mass in the separation zone shifts the shock wave towards the end of the body. As a result, the spike tip pokes through the shock wave W_1 (photo 2 and diagram 2). Here the spike tip is surrounded by supersonic flow, which forms an attached conical shock front. This front, which interacts with the wave W_1, forms a triple configuration of shock fronts (T is the intersection of the fronts in diagram 3). For a cone with $\theta = 10°$ and a flow with $M_\infty = 2.0$ [13], the inclination angle of the attached conical shock front is 31°.

In diagram 3 the inclination of the attached shock front is 52°, which corresponds to flow with $M_\infty = 2.0$ around a cone with $\theta = 35°$, which corresponds to a fluid cone which arises due to the flow separation near the spike tip. Diagram 3 shows the separating stream line, which starts from the point C_2 and coincides with the outside of the flud cone. Diagrams 2, 3, and 5 show the separation zones near the spike tip, which can be seen clearly in the corresponding photographs.

When the main shock wave W_1 is shifted along the flow from the position shown in diagram 1, supersonic flow starts to surround the spike tip. The pressure directly behind the wave is equal to the pressure for a direct shock front p_2, and the pressure at the nose part of the spike p_C is determined by the flow constriction in the conical attached shock front W_C:

$$p_c/p_\infty = \left(2\gamma M_\infty^2 \sin^2 \omega - \gamma + 1\right)/(\gamma + 1) \tag{3.1}$$

where ω is the inclination angle of the shock front to the direction of the incoming flow and γ is the adiabatic index. For sharp cones the pressure increase is insignificant; for example, for $M_\infty = 2.0$, $\theta = 10°$, and $\omega = 31°$, the pressure in the attached shock front is $p_C/p_\infty = 1.06$. The positive pressure gradient which arises interacts through the region of conical flow and leads to a separation of the laminar boundary layer at the tip of the cone. The pressure drop, which causes a similar separation at the cone, is described by an empirical formula [14] as $p_C/p_1 = 0.65 + 0.72 \cdot M_1$. In the case of a sharp spike, we can take $M_1 \approx M_\infty$, $p_C = p_1 \approx p_\infty$. According to (3.1), for $M_\infty > 1.02$, the pressure drop at the direct shock front $\omega = 90°$ exceeds the drop for which there a separation of the laminar boundary layer occurs.

The dimensions of the resultant local separation region increase because of the incoming high-velocity flow, which is limited on one hand by the side of the tangential separation starting from the triple point T and on the other hand by the shear layer which starts at the separation point C_2. In our opinion, at time $t/T_0 \approx 0.5$ pairs of toroidal vortices can exist at the end [of the cylinder], as shown between the points P_1 and C_1 and between the points P_2 and C_2. The depiction of the vortices on the diagram is dictated by the coincidence of the directions of the velocity vectors near the surfaces and between the vortices. The presence of a divergence point P_1 is related to the strong rotation of the flow near the angled edge. If the flow above the point P_1 moves from the axis and the flow left of the point P_2 moves toward the tip of the spike, the agreement of the gas motion in the region between P_1 and P_2 requires the presence of a divergence point C_1 (diagram 3).

The presence of a local separation region on the lateral surface of the cylinder, which is bounded by the separation point C_3 and the attachment point P_3, is shown experimentally for plane stationary flow around a step [12]. For pulsating flow, the formation of this local separation zone is related to the flow stages shown in diagrams 2-5. They do not show the fan of rarefaction waves, which correspond to the rotation and acceleration of the flow near the sharp edge. The terminal shock W_5, which accompanies the secondary attachment on the lateral surface of the cylinder, is observed on photo and diagram 4.

As the main shock wave W_1 displaces downward along the flow, it runs into the secondary outgoing shock wave W_2, and the two waves start to interact. The formation of the secondary shock wave W_2 is caused by the shifting shock wave W_1. The necessity of flow rotation at the end of the cylinder leads to the wave W_2. The interaction of the shock wave of one direction leads to a resultant shock wave W_3, a rarefaction wave, and contact separation [14]. The resultant wave W_3 is stronger than W_1, which can be seen from its reduced translation velocity downward along the flow. In diagram 4, the triple configuration consists of W_1, W_3, and a reflected wave W_4, where the conical wave W_C takes on a curvilinear form and now is denoted by W_1.

Because the incoming flow, which is inside a circle with its center on the tip of the spike and with a radius R_T (R_T is the distance from the axis to the triple point), enters the separation regime, its dimensions are observed to increase (diagram 4). The line of the contact discontinuity can be clearly seen, which starts from the triple point T and ends at the end [of the cylinder] at the point P_1. A curvilinear shock wave W_1 forms near the tip. The separation point C_2 from the tip slips along the lateral surface of the spike. The gas inside the separation zone is set into vortical motion. The representation of the vortical flow lines on the diagram as open spirals indicates the separation zone is filling (diagrams 3-5) or emptying (diagram 1).

As the separation zone fills, the divergence point shifts along the end surface [of the cylinder] away from the axis. Initially, the separation region fills due to the inflow of a high-pressure jet, which is limited by the separating streamline TP_1 and the separating streamline starting from the point C_2 (diagram 4). As the separation zone fills, the external boundary of the jet, which is bounded by the contact discontinuity (which starts from the tripe point T) moves from the end of the cylinder. As a result, only the inner part of the jet enters the separation zone (diagram 5). The contact surface, which starts from the flow separation point C_2, moves from the tip of the spike along the flow. A further increase in the transverse dimensions of the separation region leads to a cessation of gas inflow at the edge of the end [of the cylinder]. This closes the cycle of the autooscillation process (diagram 1). The appearance of a new triple point T near the tip (photo 5), while there is no triple shock wave configuration in photos 1 and 4, indicates some difference for different pulsation periods.

Analogous data were obtained for $M_\infty = 3.0$, $Re_\infty = 3.3 \cdot 10^6$, $\bar{d} = 0.04$, $\bar{\ell} = 0.75$, and $\theta = 10°$; the stage characteristics of the process are similar to those for $M_\infty = 2.0$. There is some difference for diagram 3, which is expressed in a stronger pressure wave, which propagates against the flow along the separation region. For $M_\infty = 3.0$, a more complex interaction of the shock waves W_1 and W_3 is sometimes observed, which is expressed in the appearance of a series of two triple points T and T'.

It should be noted that there are two maxima in the pressure on the oscillograms $p'(t/T_0)$. Their presence is accompanied by an autooscillation process of a cylinder with a sharp tip. For a blunt tip ($\theta = 45°$), this feature is not noted.

The distortion of the tangential discontinuity, which starts from the triple point T and which is clearly visible in the schlieren photographs, is explained by the pressure gradient (diagrams 3 and 4). The distortion of the outer boundary of the high-velocity jet TP_1 (diagram 4) is seen to be analogous with the results of [5], which correspond to $M_\infty = 6.0$ and are explained by the occurrence of type IV interference, which was investigated by Edni. According to [15], for $M_\infty < 3$, the Mach number is less than unity in the distorted high-velocity jet behind the front W_4 (Fig. 1b). This is confirmed for data in Fig. 1 by the fact that the internal shock front observed in [5] is not observed in the distorted annular high-velocity flow. The distortion of the annular jet flow behind the wave W_4 plays an important role in the mechanism of filling the separation zone, as shown in [5].

We note that the motion of the main shock wave W_1 relative to the pressure pulsations $p'(t/T_0)$ at the end [of the cylinder] is similar to the results in [16], where calculated relationships are presented between the behavior of the motion of the central shock front in the first cell of a supersonic nonexpanded jet, which interacts with a plane barrier, and the pressure pulsations at the barrier. In particular, the maximum outflow of the central shock front from the barrier corresponds to the minimum pressure at the barrier, which correlates well with the data presented here. In the calculated time dependence of the pressure pulsations at a point on the edge of the barrier, a local minimum is observed in the region of maximum pressure [16], which is also observed in our experiments with a spike (see Fig. 2). The correspondence in the phase relationships between the pressure pulsations and the motion of the shock front for these two types of autooscillation processes suggests similar pulsation mechanisms. Evidently one element which causes this similarity is the method of filling the separation zone by deflecting the high-pressure jet, whose external boundary coincides with the contact surface starting at the triple point.

4. The flow diagrams presented here make it possible to describe the mechanism of filling the separation zone during a single pulsation cycle. The filling starts with the formation of a separation zone near the spike tip, which includes the separation point C_2, the flow attachment point P_2, and the triple point for shock-wave interaction T (diagram 2). The distance along the axis from the end of the cylinder to the point T is denoted as $\Delta\ell$, and the distance from the point T to the axis by R_T. As discussed previously, the appearance of a local separation region near the spike tip is caused by the impossibility of the laminar boundary layer overcoming the strong increase in the pressure in the shock wave W_1.

As the shock wave W_1 displaces downwards along the flow, the local separation region increases its dimensions, which occurs due a jet flow entering into the region. The jet flow passes through the attached conical shock front W_1 and the reflected shock W_4 (diagrams 3 and 4). This method for filling the separation zone can be confirmed by comparing the mass of gas flowing into the separation zone m_1 and the gas in the zone before it is

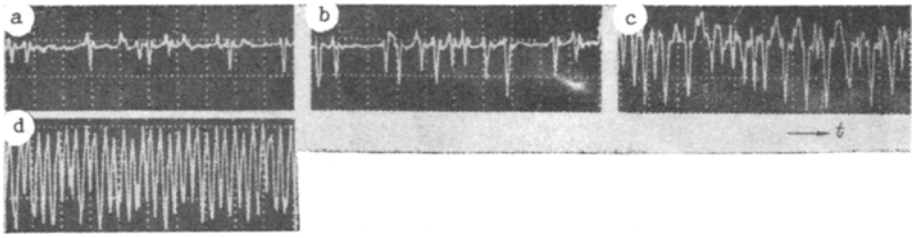

Fig. 3

evacuated. The flow entering the zone is bounded by a circle of radius R_T (diagram 4). This makes it possible to calculate the mass of gas in the separation region:

$$m_1 = \rho_\infty u_\infty \int_0^{t_f} (\pi R_T^2)\, dt,$$

where ρ_∞ and u_∞ are the density and velocity of the incoming flow, and t_f is the time for filling the separation zone. This time corresponds to the movement of the separating streamline from the cylinder. In diagram 4 this streamline is denoted by TP_1. For the regime shown in Fig. 1, the dependence of $R_T(t)$ in the interval $0 < t < t_f$ can be represented linearly:

$$R_T(t) = u_r t. \tag{4.1}$$

The maximum outflow of the main shock wave W_1 corresponds to the time $t = 0$.

On the other hand, the mass of gas in the separation regime at time t_f can be evaluated, if the volume V of the region and the density of gas in it are known: $m_2 = \int_V \rho\, dV$. For an estimate, we assume that the gas density inside the separation zone is constant and equals the gas density behind a square shock front ρ_2. The volume of the separation region at time t_f can be approximated satisfactorily by a hemisphere with a radius equal to the length of the spike.

The ratio m_1/m_2 characterizes the validity of our assumptions

$$m_1/m_2 = (\rho_\infty/\rho_2)\, u_\infty u_r^2 t_f^3/(2l^3), \tag{4.2}$$

where (4.1) is used for m_1. For $M_\infty = 2$, the radial velocity of the triple point T, which characterizes the increase in the transverse dimensions of the separation zone, is $u_r = 50$ m/sec. The time to fill the separation zone is equal to 1.03 and 0.69 msec for $M_\infty = 2$ and 3, respectively. These data are obtained by using the flow diagrams shown in Fig. 1b. The ratio ρ_2/ρ_∞ corresponds to the density increase at a square shock front. Then $m_1/m_2 = 0.9$ and 0.4 for $M_\infty = 2$ and 3. These estimates indicate the validity of the assumed mechanism for filling the separation zone. This conclusion is based on the fact that the numerical values used for the variables in (4.2) differ by a factor greater than 10^5. Therefore the resultant values of 0.9 and 0.4 can be used as a verification of this method for filling the separation zone.

The time to fill the separation zone coincides with the period of the autooscillation process. The processes of filling and emptying the separation zone for the given stages of the pulsation cycle occur simultaneously. For example, see diagram 2, which shows the presence of a local separation zone with increasing dimensions near the spike tip. However, at the same time the region behind the shock wave W_1 is emptying, which indicates that it is not sufficient simply to represent the pulsation period as the sum of intermediate times for filling and emptying the separation region.

5. One of the features of flow around a body with a spike is the existence of a regime of aperiodic pulsations. Figure 3 shows oscillograms of pressure pulsations for $M_\infty = 2.00$, $Re_\infty = 2.4 \cdot 10^6$, $\bar{d} = 0.2$, and $\theta = 20°$ (D = 80 mm). Here Figs. 3a-d correspond to spike lengths $\bar{l} = 0.52$, 0.58, 0.62, and 0.74. For $\bar{l} = 0.52$, which is somewhat larger than the distance to the outgoing shock front in the absence of a spike ($\bar{l}_s = 0.45$), we observe separate, rarely sequential, negative pressure pulses. As $\bar{l}$ increases, both the frequency and amplitude of the pulses increase (Fig. 3b). As the spike length is increased further, the

impulses follow continuously, and the amplitude reaches 50 kPa. The frequency and amplitude of the pulses fluctuates (Fig. 3c). The frequency spectrum of the pressure pulsations for regimes corresponding to Figs. 3a-c contain no discrete components. In the regime of stationary autooscillations, a distinct peak is observed in the frequency spectrum (Fig. 3d).

Analysis of the schlieren photographs, which are related to the pressure pulsation stages, showed that the relation between the position of the main shock wave and the pressure pulsation stage for the regime of aperiodic pulsations is similar overall to the relationship for the regime of developed autooscillations. The appearance of aperiodic pulsations is explained by the fact an insignificant thrust of the spike tip behind the shock wave leads to a loss of stability of a given oscillatory system, before sufficiently effective feedback exists. An analogous phenomenon was observed for jet systems [17]. The impulsive nature of the occurrence of strong pulsations at their zone boundary indicates a relaxation character of the autooscillations. This is inferred by the fact that the autooscillation amplitude increases from a small value to its steady-state value over a half-period of the oscillations.

LITERATURE CITED

1. W. Calarese and W. L. Hankey, "Modes of shock-wave oscillations on spike-tipped bodies," AIAA J., 23, No. 2 (1985).
2. J. S. Shang, R. E. Smith, and W. L. Hankey, "Flow oscillations on spike-tipped bodies," Paper/AIAA, N 80-0062, Pasadena, Calif. (1980).
3. G. F. Glotov, "Features of supersonic flow around blunted bodies with a spike," Aviation Engines, Trans. of the 8th Scientific Convention on Cosmonautics [in Russian], Nauka, Moscow (1986).
4. L. Ériksson, "Flow pulsations on convex conical nose parts," RTK, 16, No. 11 (1978).
5. A. G. Panaras, "Pulsating flows near axisymmetric convex bodies," RTK, 19, No. 8 (1981).
6. A. N. Antonov and V. K. Gretsov, "Investigation of transient separated supersonic flow around bodies," Izv. Akad. Nauk SSSR, Mekh. Zhidk. Gaza, No. 4 (1974).
7. V. I. Zapryagaev and S. G. Mironov, "Experimental investigation of pulsations in the forward separation zone for supersonic flow velocities," Zh. Prikl. Mekh. Tekh. Fiz., No. 4 (1989).
8. P. S. Panda, Autooscillations in Systems with a Finite Number of Degrees of Freedom [in Russian], Nauka, Moscow (1980).
9. I. I. Volonikhin, V. D. Grigor'ev, V. S. Dem'yanenko, et al., "Supersonic wind tunnel T-313," in: Aerophysical Investigations [in Russian], ITPM SO AN SSSR [Institute of Theoretical and Applied Mechanics of the Siberian Department of the Academy of Sciences, USSR], Novosibirsk (1972).
10. V. I. Zapryagaev and S. G. Mironov, "Methodology of tying flow-field photography to measurements of local parameters," in: Methods of Aerophysical Investigations: Proc. of the 4th All-Union Conference on Methods of Aerophysical Investigations [in Russian], ITPM SO AN SSSR, Novosibirsk (1987).
11. V. I. Zapryagaev, "Investigation of pulsations of the separation zone of a free cavity for supersonic flow," Zh. Prikl. Mekh. Tekh. Fiz., No. 6 (1985).
12. A. A. Zhelotovodov, É. Kh. Shilein, and V. N. Yakovlev, "Development of a turbulent boundary layer under conditions of mixed interaction of shock waves and rarefaction waves," Preprint No. 28-83 [in Russian], ITPM SO AN SSSR, Novosibirsk (1983).
13. Yu. A. Kibardin, S. I. Kuznetsov, A. N. Lyubimov, and B. Ya. Shumyatskii, Atlas of Gas-Dynamic Functions for Large Velocities and High Temperatures of Air Flow [in Russian], Gosénergoizdat, Moscow–Leningrad (1961).
14. V. Ya. Borovoi, Flow of Gas and Heat Transfer in the Zone of Interaction of Shock Waves with a Boundary Layer [in Russian], Mashinostroenie, Moscow (1983).
15. R. Courant and K. Friedrichs, Supersonic Flow and Shock Waves [Russian translation], IL, Moscow (1950).
16. V. N. Uskov, V. V. Tsymbalov, and E. N. Tsymbalova, "Numerical solution of the problem of a transient interaction of a supersonic jet with a barrier," Model. Mekh., 1(18). No. 6 (1987).
17. Yu. V. Serov and A. V. Sobolev, "Investigation of pulsations during the interaction of expanding jets with plane barriers," Proc. of a Symposium on the Physics of Acoustic Hydrodynamic Phenomena, Sukhumi [in Russian], Nauka, Moscow (1975).